

# Proteomic Tools to Characterize Non-Thermal Plasma Effects in Eukaryotic Cells

K. Wende<sup>1,2\*</sup>, A. Barton<sup>1,2</sup>, S. Bekeschus<sup>1,2</sup>, L. Bundscherer<sup>1,2</sup>, A. Schmidt<sup>1,2</sup>, K.-D. Weltmann<sup>2</sup>, & K. Masur<sup>1,2</sup>

<sup>1</sup>Center for Innovation Competence (ZIK) *plasmatis*, Felix-Hausdorff-Str. 2, 17489 Greifswald, Germany; <sup>2</sup>Leibniz Institute for Plasma Sciences and Technology e.V. (INP), Felix-Hausdorff-Str. 2, 17489 Greifswald, Germany

\*Address all correspondence to: K. Wende, Address; Tel.: +49-3834-5543923 ; Fax: +49-3834-554301; Email: kristian.wende@inp-greifswald.de

**ABSTRACT:** Plasma medicine is an exciting new scientific field due to recent developments in nonthermal physical plasmas operating at atmospheric pressure. In the present study, the effect of an argon-operated plasma jet (kINPen) using either humidified or dry argon as the working gas was investigated on human keratinocytes with respect to changes in the cellular protein expression pattern. The possibility of characterizing the plasma source by its effects on the cell model was tested. After successfully establishing the gel-free proteomics approach using liquid chromatography–high-resolution mass spectrometry, a data set of 3,818 different human proteins from all cellular compartments and protein classes was analyzed. Overall, 10% of proteins were regulated by the plasma treatment, indicating a strong effect of the plasma on the human cell. While there is only weak evidence for direct protein modification, plasma does trigger the active translation of stress-responding proteins. Among the most regulated proteins, cytoskeletal components (keratins), chaperones (heat shock proteins), and proteins involved in oxygen turnover (oxidoreductases, NQO1) were found. Therefore, the presence of reactive oxygen species as well as an organized cellular response are indicated, emphasizing the need for further research in medical applications. Additionally, our approach enables the differentiation between the two selected plasma parameters, allowing its further use to identify key players both in plasma-treated liquids and cellular response. This study and the methodology described herein can be used as a basis to further address the underlying mechanisms of plasma–cell interactions. The data obtained will facilitate fundamental understanding on cellular responses after plasma stimulation.

**KEY WORDS:** keratinocytes, plasma medicine, non-thermal atmospheric pressure plasma, plasma jet, proteomics, reactive oxygen species, LC/MS

## I. INTRODUCTION

The first plasma treatments of living tissue date back to the beginning of the 19<sup>th</sup> century (i.e., violet rays and the carbon arc lamp), but they have never played a significant role, mainly due to a lack of basic understanding and unrealistic promises regarding several medical indications. The instant generation of reactive species, of which many play key roles in cell biology, combined with the synergistic physical effects of plasma radiation and electromagnetic fields, have recently led to new therapeutic methods, for example, in chronic wound healing.

Nonthermal atmospheric pressure plasmas have made a developmental leap in the last decade, triggering the evolution of new biomedical tools, and they offer applicability for different medical issues.<sup>1,2</sup> Due to their excellent compatibility with heat-sensitive material, the use of non-thermal plasmas to modulate processes in living matter has come into focus. Reportedly, non-thermal plasmas do induce different effects in living biological systems. The killing of microorganisms and, more recently, cancer cells have been well described.<sup>3,4</sup> The inactivation of bacteria in the presence of eukaryotic cells by argon plasma has been shown *in vitro*.<sup>5,6</sup> The general applicability to treat the skin or infected wounds *in vivo* has also been investigated.<sup>7,8</sup>

Sublethal effects in eukaryotic cell systems include changes in cycle progression, alteration of DNA integrity, and changes in membrane molecules.<sup>9–11</sup> Plasmas are gas-like systems that are distinguished from an ordinary gas by the presence of charged particles. Nature, frequency of occurrence, and energy of these particles determines the plasma properties. After ignition, the plasma forms a variable mixture of active components: electrons, ions, radicals, reactive molecules, as well as different types of radiation, including electric fields and ultraviolet radiation.<sup>12,13</sup> During non-thermal plasma discharges, reactive oxygen species (ROS) and reactive nitrogen species (RNS), including singlet oxygen, superoxide anion radical, ozone, hydroxyl radicals/hydrogen peroxide (H<sub>2</sub>O<sub>2</sub>), and nitrous oxide (NO), have been observed.<sup>14,15</sup> Although a generally accepted mechanism of action is still missing, reactive oxygen and nitrogen species (ROS/RNS) have been assigned a major part.<sup>16</sup> Some of these (H<sub>2</sub>O<sub>2</sub>, NO) are well-known signal-transducer molecules in cell biology that trigger cell differentiation or immune responses, or that regulate angiogenesis.<sup>17,18</sup> ROS/RNS fluxes and distribution strongly differ between sources and process parameters (e.g., working gas composition), facilitating the opportunity to tailor a plasma's efficacy and target structure.<sup>19</sup>

Although the body of information on the biological effects of plasmas is growing, a thorough biological characterization of atmospheric plasma-triggered effects is needed. To decipher the complex mechanism of how eukaryotic cells/tissues react on the exposure to plasmas, in-depth analysis of the responses is necessary, and this can be achieved using high-content methods like transcriptomics and proteomics.<sup>20</sup> Ideally, this approach should lead to the identification of a robust “biomarker” that allows easy but specific detection *in vitro* and *in vivo*.

The aim of this study was to examine the dimension of the biological effects of an argon plasma jet at atmospheric pressure (kINPen09) on human keratinocytes using two selected treatment regimens (dry vs. humidified argon working gas). Different types of ROS, especially hydroxyl radicals, have been detected in the gaseous plasma effluent.<sup>15</sup> However, only limited data are available regarding its influence on eukaryotic cells.<sup>5,10</sup> The HaCaT cell, a well-established *in vitro* model for human keratinocytes, has been used previously. These studies show a behavior typical for eukaryotic cells such as sensitivity toward nutrition deprivation or the ability to undergo apoptosis. HaCaT cells behave like normal keratinocytes in terms of stratification at an air interface, migration, and production of keratins 1 or 14, depending on their developmental progress.<sup>21</sup>

Effects on the total cellular proteome were investigated using liquid chromatography high-resolution mass spectrometry.

## II. MATERIAL AND METHODS

### A. Cell Culture

Adherent human keratinocytes (HaCaT), purchased at DKFZ Heidelberg (Germany), were cultured in an incubator (37°C, 5% CO<sub>2</sub>, 95% humidity) using Roswell Park Memorial Institute 1640 medium supplemented with 8% fetal calf serum and 1% penicillin/ streptomycin (complete RPMI). Cells were used for 30 passages only and were subcultured twice weekly using standard procedures.<sup>22</sup> To prepare the experiment per the desired reading point,  $1 \times 10^6$  HaCaT cells were seeded in a 60-mm dish using complete RPMI and were allowed to rest for 24 h in an incubator. All experiments were performed in triplicate.

### B. Plasma Treatment

In this study, an atmospheric-pressure non-thermal plasma source was used (kINPen09, neoplas tools GmbH, Greifswald, Germany) that is identical to the device used in related studies concerning the impact on mammalian cells (Fig. 1). The plasma jet consisted of a centered rod electrode inside a ceramic capillary and a grounded ring electrode.<sup>13,23</sup> The working gas was argon (Argon N50, Air Liquide) with a gas flow rate of 3 standard liters per minute (slm). When a sinusoidal voltage signal 2–6 kV<sub>pp</sub> with a frequency of ~1 MHz was applied to the centered electrode, plasma ignited in the core region, producing effluent approximately 12 mm long  $\times$  2–3 mm wide. Humidification of the argon gas

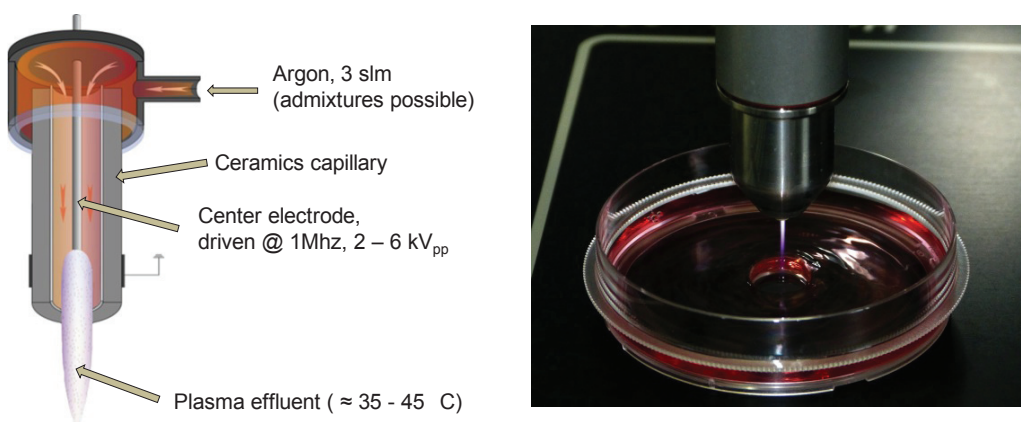


**FIG. 1:** Schematic setup and photography of the kINPen09 plasma source. The culture dish with cell culture medium was placed 13 mm distant from the jet nozzle, and the jet moved in a meandering pattern over the whole dish.

was achieved as described earlier using a bubbler setup (dry conditions: 25 ppm H<sub>2</sub>O, humid conditions: 300 ppm H<sub>2</sub>O).<sup>24</sup>

Plasma treatment was performed as an indirect treatment regimen using a motorized stage. Complete RPMI was treated in triplicate for 240 s in 60-mm dishes with the plasma jet. Only the cell culture medium came into contact with the active plasma. Subsequently, the cell culture medium was transferred immediately into the dishes containing cells and kept in an incubator for an appropriate period of time (3 h, 6 h, and 24 h) before harvest. The control cells (“0 s”) were not exposed to plasma but were otherwise treated identically. Alternatively to plasma treatment, 50 μM H<sub>2</sub>O<sub>2</sub> was used as control. HaCaT cells were harvested by cell lysis using RIPA buffer (1% Igepal CA-630, 0.5% sodium deoxycholate, 0.1% sodium dodecyl sulphate, 2 mM EDTA, protease inhibitor cocktail) 3 h, 6 h, and 24 h after plasma treatment. After washing with ice-cold PBS, 200 μl RIPA buffer was added. Cells were collected using a cell scraper, and the obtained suspensions were sonicated on ice. After clearance by centrifugation (10,000 ×g, 4°C), supernatant was used for further analysis.

### C. Protein Separation and Digestion

After protein quantification (RC DC assay, microfuge tube protocol with reagent S, Biorad), protein concentration was adjusted to contain 1 mg/ml with RIPA buffer. After adding an appropriate amount of 5× running buffer (0.25 M TRIS, 0.35 M SDS, 1.4 M 2-mercaptoethanol, 0.3 mM bromphenol blue in 40% glycerol/water) and protein denaturation (5 min, 95°C), 30 μg protein per sample was fractionated according protein mass by SDS gel electrophoresis (ProGel Tris Glycerin 10%) for 120 min/125 V in electrophoresis buffer (20 mM TRIS; 200 mM glycine, 3.5 mM SDS, pH 8.3). After washing (2× 2 min, Millipore water) and fixation for 20 min in methanol:water:acetic acid (50:40:10), gel was stained using Coomassie for 1 h. Subsequently, gel was washed and cut into lanes that were divided into 12 fractions. After destaining, in-gel protein digestion was performed using sequencing grade trypsin (10 μg/ml in 0.05 M (NH<sub>4</sub>)<sub>2</sub>CO<sub>3</sub> buffer Promega, Mannheim, Germany) overnight at 37°C. After peptide extraction from the gel pieces using a step gradient of formic acid/acetonitrile and concentration/acetonitrile removal (aqueous settings, SpeedVac Concentrator, Eppendorf, Hamburg, Germany), the peptide mixture was subjected to liquid chromatography/mass spectroscopy.

### D. Liquid Chromatography/High-Resolution Mass Spectrometry

The peptide mixture obtained as outline in the previous section was subsequently analyzed by nanoliquid chromatography–high-resolution mass spectrometry. Samples were analyzed using a Proxeon nanoLC II (Thermo Fisher Scientific) injecting 2 μl of sample on a 30-cm (75-μm inner diameter) fused silica column (Aeris, 3 μm diameter RP18 material, Phenomenex, Aschaffenburg, Germany). Separation by polarity was achieved using a water 0.1% acetic acid/acetonitrile 0.1% acetic acid gradient (0.3 μl/min) over 120 min. Subsequently, eluent was ionized using an electrospray ionization technique

(NanoSpray III source). High-resolution mass spectrometry was performed with an AB-scix TripleTOF 5600 mass spectrometer in information-dependent acquisition (IDA) mode. Parental masses were obtained from all ionized fragments ( $m/z$  400–2000); daughter ion masses were obtained only from significantly abundant fragments. Rolling collision energy for fragmentation ( $m/z$  400–1250) was used. Autocalibration using 2  $\mu$ l *Saccharomyces cerevisiae* enolase 1 tryptic digest (Waters, Manchester, United Kingdom) was performed every three runs. All samples were injected twice.

Raw data were then analyzed for peptide and protein identification using ProteinPilot 4.5 software (Paragon algorithm), searching against the latest UniProt human complete protein dataset with search effort set to “thorough.” This search mode allows the detection of proteins in unknown protein modifications (PTMs), whereas the “fast” setting takes only standard PTMs into account. One missed cleavage was allowed in the search. Group files with identified proteins were used in PeakView software (MicroQuantitation App) for relative quantification. After normalization in MarkerView, further data processing to obtain information on protein expression pattern and statistical analysis was performed by Partek Genomic Suite, PANTHER database, and Ingenuity Pathway Analysis (IPA). To analyze significant changes in protein abundance using Partek, we grouped all related time points (control/humid/dry/ $H_2O_2$ ) together, yielding three data points with the absolute reading (area under curve \* time) per protein and treatment.

### III. RESULTS AND DISCUSSION

The effects generated by a nonthermal atmospheric-pressure argon-based plasma jet on the cellular proteome of eukaryotic cells were characterized. Human HaCaT keratinocytes were used as a model cell line for eukaryotic cells with additional relevance to wound-healing processes. A workflow for the investigation of the human proteome was established and used to analyze the influence of two different plasma parameters (dry and humid process gas) on the model cell system. Previously, a distinct impact of argon gas humidification on plasma chemistry and cell viability had been identified by our group.<sup>24</sup>

A nanoliquid chromatography–high resolution mass spectrometry (nLC/HRMS) procedure was successfully established. The core components of the workflow were (1) the complexity reduction of the cell lysate by one-dimensional (1D) gel electrophoresis; (2) the in-gel digestion of the separated proteins; and (3) the nano-LC, which allowed very small analyte amounts to be analyzed (Fig. 2). Without 1D gel separation, only 40–50% of the proteins were identified because of co-elution and peptide masking (data not shown). A resolution of approximately 22,000 was achieved, while mass error was approximately 1–3 ppm. Between 1,500 and 2,100 different human proteins with a quality score  $\geq 2$  (at least one unique peptide per protein, confidence > 99%) were identified by ProteinPilot software (Paragon algorithm) in each sample (0.1–1  $\mu$ g protein digest on column). Subsequently, the relative abundance of these proteins was calculated by PeakView software. The measured protein abundances span 4 to 5 log steps, allowing a good quantitative read out. The lowest detected protein (PTPLAD1, 6000 counts\*time) was approximately 4.9 log steps less intense than SHC1 (359  $10^6$  counts\*time). A total

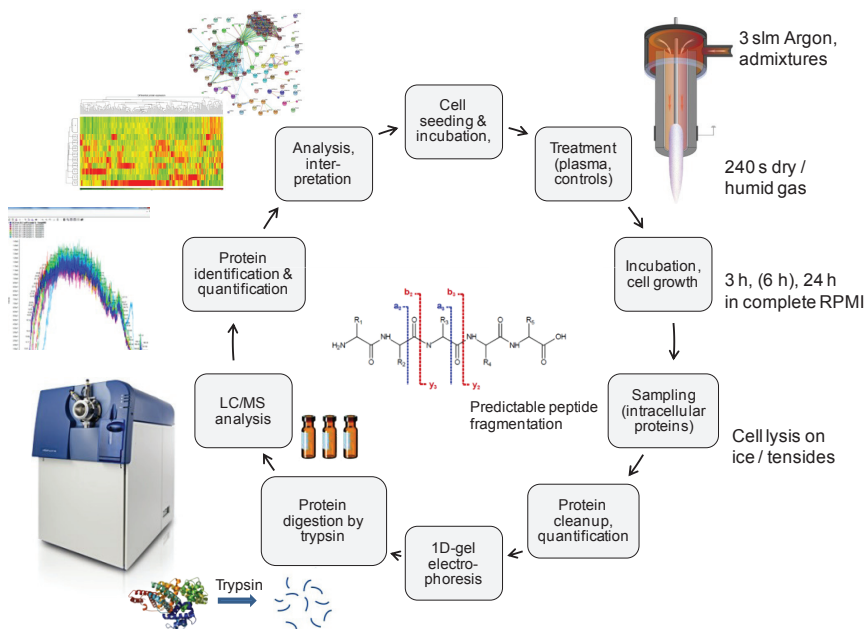


**FIG. 2:** Setup of whole experimental process, further details as described in the text. The central element of the procedure is the predictable fragmentation of the peptide bond under mass spectrometry conditions. It allows the identification of the peptides which were obtained by the protein digestion using ProteinPilot software. Consequently, peptides were assigned to the corresponding proteins. Data analysis using Ingenuity Pathway analysis, PANTHER database, and String database allowed conclusions on cell physiology under the tested conditions.

of 2500 proteins (65%) were between  $1 \times$  and  $10 \times 10^6$  counts\*time. However, only 25–35% of acquired MS spectra were used for protein identification. The remaining spectra could not be assigned to a specific amino acid/amino acid sequence by the software. This effect is typical in mass spectrometry-based proteomics and does not reflect on protein modifications generated by the plasma. Rather, it emphasizes the need of more sophisticated software tools to utilize the measured raw data.<sup>25</sup> In addition to general protein identification, the Paragon algorithm also allowed the detection of amino acid modifications (e.g., methionine S-oxidation, deamidation etc.). Only a negligible difference in number and type of modification was observed between control and plasma-treated cells. This result indicates that differences in the cellular proteome can instead be explained by a regulated cell response rather than random protein damage. However, as total identified protein numbers are somewhat lower for plasma-treated cells (1,900 vs. 2,100 in control), protein oxidation and similar processes cannot be excluded ultimately. Additionally, a loss of function of isolated and dried proteins has been described after long-duration plasma treatment using a He/O<sub>2</sub> jet.<sup>26</sup> However, the impact of this finding on the situation of proteins in mammalian cell culture or tissue in which a water-dominated physiologic environment dictates conditions (e.g., euhydic

pH, isotonic osmolarity, and standard ion strength) might be limited, as is indicated by our results. Clarification will be left for future research focusing on plasma-generated protein modifications under physiologic conditions.

In the described setup (12 different samples in duplicate), a total of 3800 different proteins (with score  $\geq 2$ ) could be detected, belonging to 28 different classes of proteins (Figs. 3 and 4). This number of proteins reflects a typically achievable data depth and is influenced by lab conditions, cell line, instrumentation, and software. It is commonly estimated in systems biology that around 10,000 different proteins are expressed within a cell; however, some have a very low copy number.<sup>27</sup> In our approach, the abundance of roughly 10% was affected by the plasma treatment (humid and/or dry working gas, all time points); it increased for 411 proteins and decreased for 339 proteins (Fig. 3). Analyzing different expression in terms of quantitatively different abundance using Partek yielded 160 proteins, indicating a significant difference between control and humid plasma treatment (up or down). When these proteins were clustered using the hierarchical clustering tool in Partek (Fig. 4), a certain pattern was observed: most differences compared to the control were found for humid plasma-treated cells (bottom three lines, reflecting condition 3 h, 6 h, and 24 h after treatment), while cells treated with dry plasma showed more similarities to the control. However, protein expression was still altered profoundly more strongly than after H<sub>2</sub>O<sub>2</sub> treatment, which triggered a moderate change in protein expression only (top 3 lines). All controls are located in the center in one group, indicating high similarity within. However, this low number of identified changes reflects only the most robust alterations in protein expression and underestimates the actual changes observed. For example, when we analyzed for exclusively changed proteins (fold ratio  $> 2 / < 0.5$ ) after dry or humid plasma treatment by pivot table data analysis, we found an increased abundance for 216/178 proteins

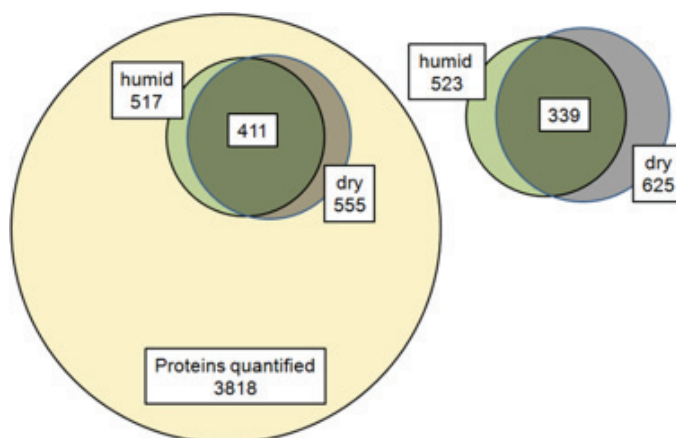


**FIG. 3:** Of 3818 proteins detected and quantified (large circle), 411 proteins were found upregulated (left insert) and 339 proteins were downregulated (right) under the plasma condition and incubation time tested. Expression of 100–200 proteins was affected by dry or humid plasma treatment exclusively. Circle diameters are to scale.

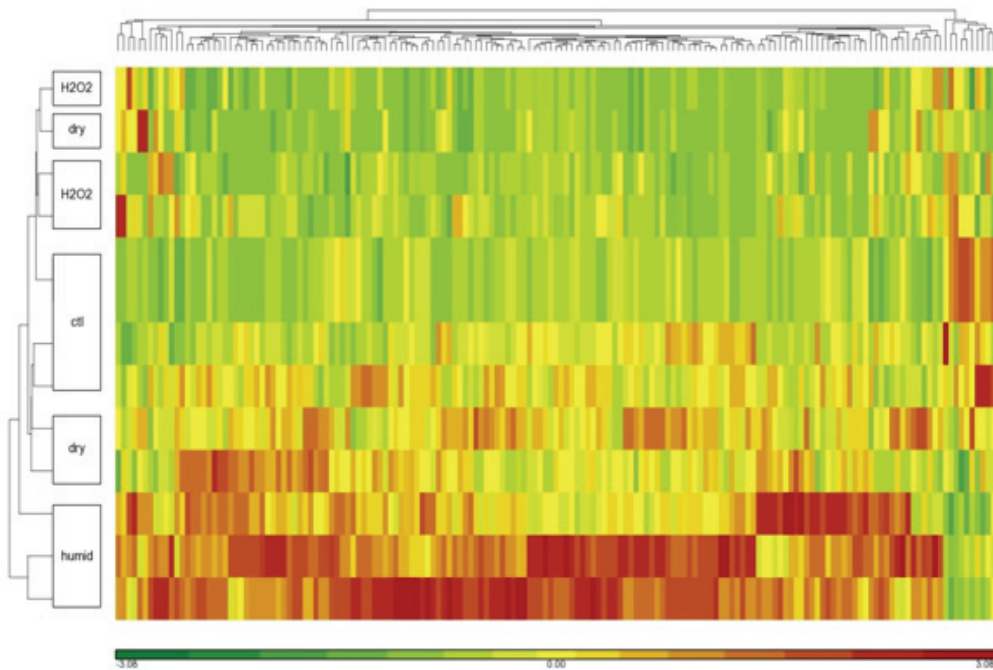


**FIG. 4:** Hierarchical clustering indicates changes in HaCaT cells, the protein expression pattern between control, dry argon plasma, humid argon plasma, and hydrogen peroxide–treated cells (Partek software, based on comparison of humid plasma treatment versus control group). A high grade of similarity within humid plasma group is indicated, while stronger distinction from control and dry plasma treatment is discernible.

(dry/humid) and a decrease in 214/112 cases (dry/humid), respectively. Together, these findings indicate that humid plasma treatment exerts a higher impact on the protein abundance in absolute measures but in a (slightly) lower number of proteins, whereas dry plasma treatment exerts a lower impact on the protein abundance in absolute measures but in a higher number of proteins. Observing the composition of the exclusively changed proteins after dry or humid treatment in terms of GO annotation, differences between humid and dry treatment appear to be of quantitative rather than qualitative nature (Fig. 5). Hence, both treatment types are essentially the same and differ mainly in the extent of the effect. Recent findings underscore this observation as being related to hydrogen peroxide, in which production rate increases with increasing operation gas humidity in plasma.<sup>24</sup> Thus, the general changes in the cellular proteome observed are discussed together herein.

Although it was not possible to detect all presumably present proteins, the obtained data allowed conclusions regarding cell physiology after plasma treatment. Using the PANTHER database, two-thirds of the observed proteins could be annotated according to protein class or biological function (Fig. 6). The highest numbers of proteins identified belong to nucleic acid binding proteins (520, histones etc.), emphasizing the



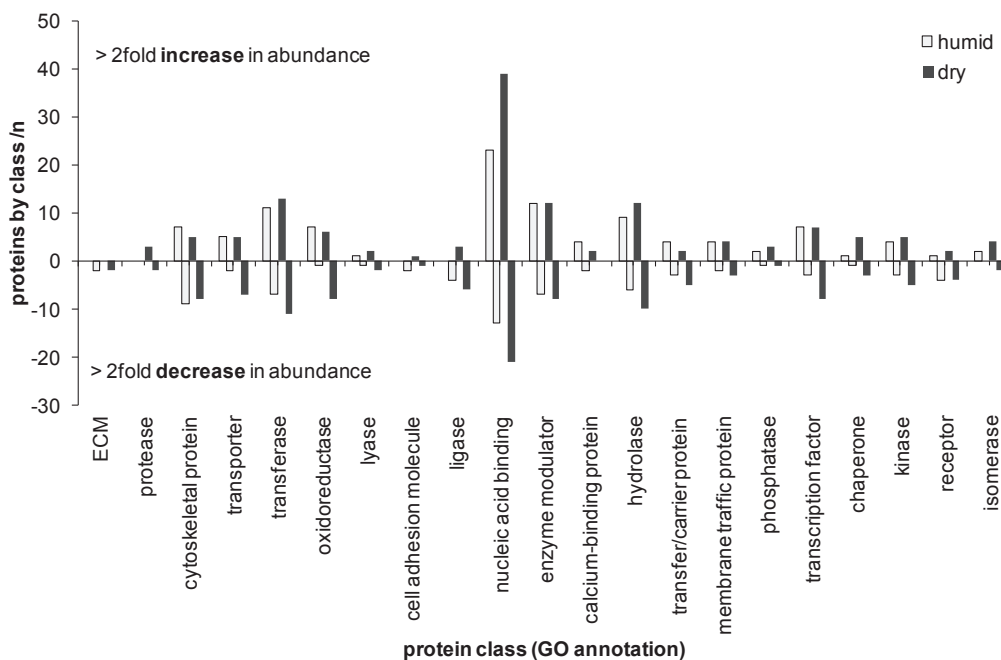


**FIG. 5:** Numbers of proteins exclusively changed after humid or dry plasma treatment according to the GO protein classification. Of 2,661 annotated proteins, abundance of 126/150 proteins increased and abundance of 77/116 proteins decreased, respectively (humid/dry treatment). Overall, behavior after dry or humid treatment was similar; however, the extent of the respective changes differed between dry (=mild) and humid (=intense) treatments (see also Fig. 8).

important role of DNA conservation in human cells. This abundance also indicates the very active nucleus of HaCaT cells and the functional ribosomal protein translation machinery. This finding was confirmed by Ingenuity pathway analysis (IPA®) of the dataset, which identified functional signaling by the eukaryotic initiation factors eIF4 and eIF2 to be among the top canonical pathways (76 of 159 and 103 of 182 related proteins, respectively). In particular, the eIF4 pathway can interfere with both intracellular and extracellular stimuli transmitted via mitogen-activated kinases (MAPK, e.g., ERK1/2, p38, etc.) and is responsible for ribosomal protein translation.<sup>28</sup> The functionality (and activation) is reflected by the increased abundance of ROS handling proteins and is indicative of stimulation in general (e.g., for cytokine expression, which has been seen in HaCaT keratinocytes). Cytoskeletal, structural, or cell-membrane-bound adhesion molecules were also numerous ( $\approx 300$ ). Other membrane-associated proteins like receptors (71) were detected, indicating that cell membranes were solubilized by the RIPA buffer. A large group of proteins belongs to the primary metabolism (glycolysis, citrate cycle etc.,  $\approx 500$ ). When analyzing the annotated proteins (2,661, 70% of detected proteins) for specific enrichment after plasma treatment (Fig. 5), enrichment was found for chaperones (HSP27, 70, and 90), cytoskeletal and structural proteins (overrepresented

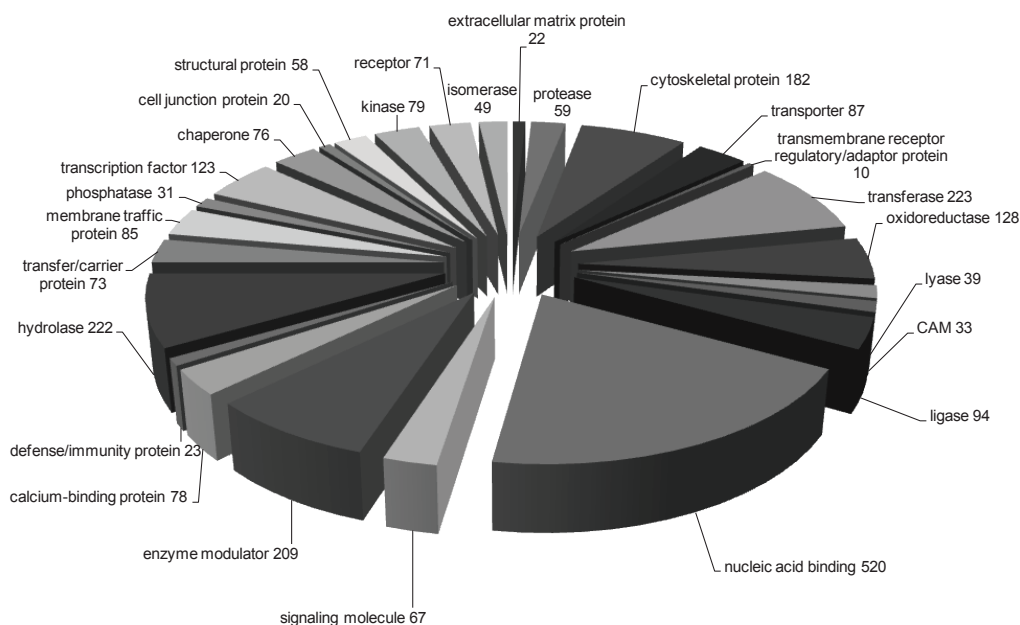


**FIG. 6:** Protein class annotation of proteins identified and quantified by LC-MS. 2,661 of 3,818 proteins could be categorized in the PANTHER database (70%). Cytosolic, membrane-bound, and nuclear-associated proteins of broad spectrum of protein classes were detected. The greatest numbers of proteins belong to nucleic acid binding proteins (520) and energy metabolism and cytoskeletal proteins (182).

in proteins with increased abundance), and different enzyme classes (overrepresented in downregulated proteins). Nucleic acid-binding proteins, enzyme modulators, and oxidoreductases were up- or downregulated in overall comparable numbers, indicating limited or absent effects in these groups.

Among the proteins with increased abundance at all time points and regardless of operation gas humidity, the heat shock proteins (HSPs) stood out with a very robust and profound increase in expression. These proteins are observed after cellular stresses of different origins and serve mainly to prevent misfolding or aggregation of cellular proteins,<sup>29</sup> preventing cell death. The small HSP27 and the medium-sized HSP70 are usually found in low abundance under physiologic conditions, but they are strongly inducible. However, the temperature during treatment never exceeded 37°C (unpublished data). Hence, HSPs were triggered most likely by ROS-transmitted effects. Obviously, H<sub>2</sub>O<sub>2</sub> is able to cross the cell membrane and to increase the intracellular ROS pool, as has been detected after kINPen treatment of mammalian cells.<sup>30</sup> Other processes like oxidation of membrane lipids may be involved. Subsequently, HSP production may also be triggered by secondary messengers with oxidative properties.<sup>31</sup> It has been shown that the application of cytotoxic stimuli, delivered below a threshold level, can elicit protective responses by overexpression of HSPs.<sup>32</sup> Translated to plasma medicine, this

finding indicates that a low-level plasma treatment (e.g., of wounds) may brace the cells to withstand prolonged inflammatory situations caused by bacteria or immune response. The positive outcome of a wound-healing study using plasma treatment may be in part explained by this effect.<sup>7</sup> In the present study, the role of reactive species and their effects in mammalian cells has been further emphasized by the use of gene ontology annotation (biological function: active on “external stimulus”). In our analysis, many proteins belonging to cellular oxygen handling were present in the dataset. Among the proteins with increased expression levels were peroxiredoxins, thioredoxins, superoxide dismutase (SOD), and NAD(P)H dehydrogenase [quinone] 1 (NQO1), all of which demonstrate evidence that plasma activated nuclear receptor–related factor 2 (NRF2) signaling. Although the total number of regulated oxidoreductases does not change with humid or dry working gas plasma treatment (Fig. 7), single proteins of this class show a specific pattern (Fig. 8). Overall, the relative abundance of these proteins increases with incubation time after plasma treatment. Differences were also found between humid and dry plasma conditions, although no obvious pattern was detected, probably due to the similarity of both treatments, as had already been discussed. Taken

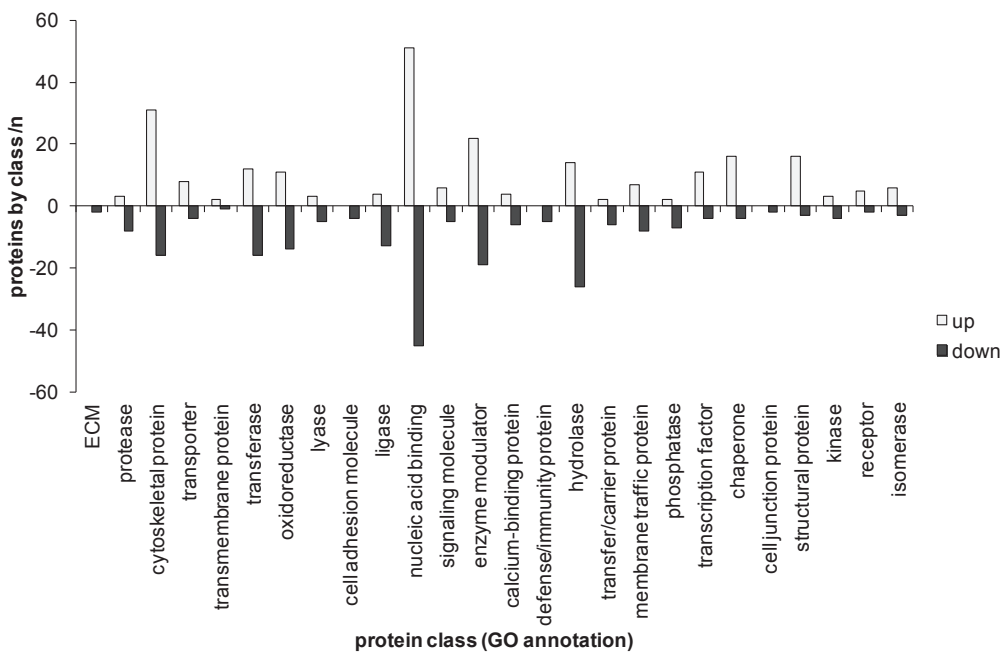


**FIG. 7:** Overview of the plasma treatment effect in HaCaT cells: humid or dry treatment, numbers of proteins with higher (up, 411 in total) or lower (down, 339 in total) abundance. Of 2,661 annotated proteins, the highest enrichments were found for chaperones, cytoskeletal and structural proteins (overrepresented in proteins with increased abundance), and different enzyme classes (overrepresented in downregulated proteins). Nucleic acid binding proteins, enzyme modulators, and oxidoreductases were up- or downregulated in comparable extents.

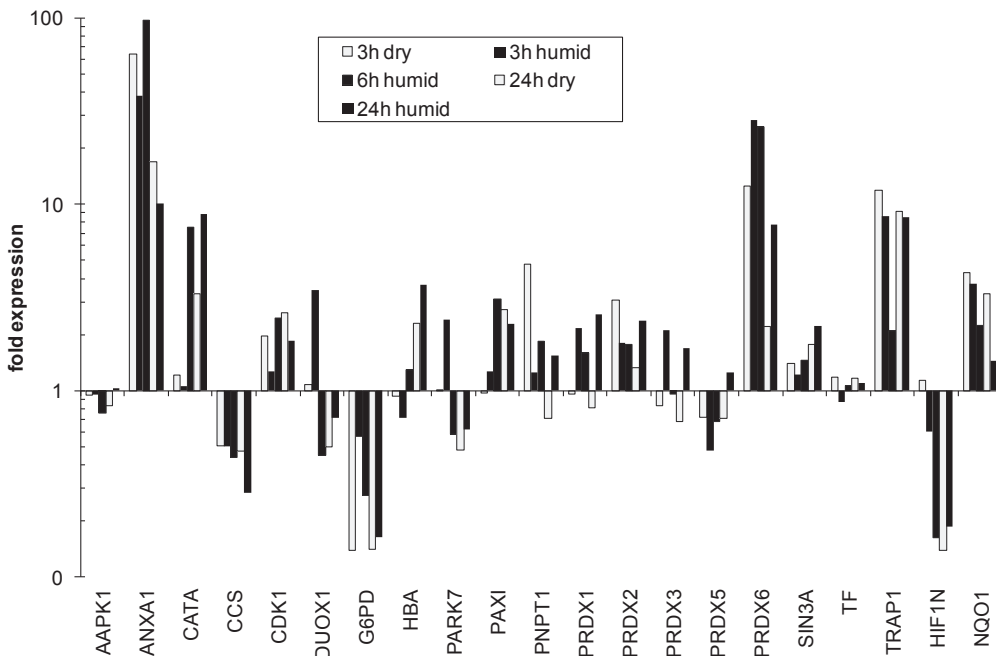


**FIG. 8:** Proteins with annotation “oxidative stress.” Abundances changed after plasma treatment, both increasing and decreasing. The greatest increases in abundance occurred for annexin (ANXA1) and peroxiredoxin 6 (PRDX6), the greatest decreases in abundance occurred for glucose-6-phosphate dehydrogenase (G6PD) and HIF1N. Intense treatment (humid, black bars) showed mostly higher intensity changes than milder (dry) treatment.

together, both HSP expression and the oxidoreductase/NRF2-related pattern indicate an increased abundance of intracellular reactive species (ROS and/or RNS), which needs to be controlled by the cell. However, as ROS do play roles as signaling molecules using specific pathways, further (and direct) impact on cellular behavior is likely, for example, via epidermal growth factor receptor (EGFR) or secreted proteins such as interleukins and growth factors.<sup>33,34</sup> An interesting role seems to be taken by different cytoskeletal proteins (6.8%, 182 proteins), especially by the keratins, which are highly abundant in this cell line. Research elucidating their role in cytoprotection and cellular development after plasma treatment is currently under way.

#### IV. CONCLUSION

In the present study, the influence of an atmospheric-pressure argon-based plasma jet (kINPen09) on human keratinocytes was investigated. Using liquid chromatography–mass spectrometry, the cellular proteome was analyzed in respect to plasma-related changes in expression pattern or protein modifications. Two differently operating gas parameters influencing plasma chemistry were used: dry and water-enriched (humidified) argon.

After successfully establishing the gel-free proteomics approach, 3800 human proteins from all cellular compartments and protein classes were detected. Although there is only weak evidence for direct protein modifications, plasma triggered the translation of oxidative stress responding proteins and influenced cell cycle regulatory proteins and protein translation. The results clearly show a strong effect of the plasma jet on the human cell, reflected by its proteome. Overall, approximately 10% of proteins were found to be regulated after plasma treatment. Proteins showing the most interesting behavior were cytoskeletal proteins, chaperones like heat shock proteins, and oxygen-handling enzymes related to a NRF-2 orchestrated response. This indicates the presence of oxidative stress due to the plasma generated ROS but also an organized cellular response to it, thereby encouraging further research in medical application for skin-related disorders.

Additionally, the approach enables the differentiation between the two selected operating gas parameters used, allowing the further use of this technique to identify key players both in plasma-treated liquids and in cellular response. This study and the methodology described herein can be used as a basis on which to further address the underlying mechanisms of plasma–cell interactions and to enable the specific recognition of both active plasma components and biological key players (biomarkers).

## ACKNOWLEDGMENT

The authors gratefully acknowledge the work of Liane Kantz (ZIK plasmatis), Prof. Dr. Dörte Becher, and Sebastian Grund (University of Greifswald). Special thanks are due to Marcel Jarick for the careful sample preparation. This work was supported by the German Federal Ministry of Education and Research (BMBF), grant number 03Z2DN11.

## REFERENCES

1. Weltmann KD, von Woedtke T. Basic requirements for plasma sources in medicine. *Eur Phys J-Appl Phys*. 2011;55(1).
2. Laroussi M. Low-temperature plasmas for medicine? *IEEE T Plasma Sci*. 2009;37(6):714–25.
3. Vandamme M, Robert E, Lerondel S, Sarron V, Ries D, Dozias S, Sobilo J, Gosset D, Kieda C, Legrain B, Pouvesle JM, Le Pape A. ROS implication in a new antitumor strategy based on non-thermal plasma. *Int J Cancer*. 2012;130(9):2185–94.
4. Laroussi M. Nonthermal decontamination of biological media by atmospheric-pressure plasmas: review, analysis, and prospects. *IEEE T Plasma Sci*. 2002;30(4):1409–15.
5. Wende K, Landsberg K, Lindequist U, Weltmann KD, von Woedtke T. Distinctive activity of a nonthermal atmospheric-pressure plasma jet on eukaryotic and prokaryotic cells in a cocultivation approach of keratinocytes and microorganisms. *IEEE T Plasma Sci*. 2010;38(9):2479–85.
6. Brun P, Brun P, Vono M, Venier P, Tarricone E, Deligianni V, Martines E, Zuin M, Spagnolo S, Cavazzana R, Cardin R, Castagliuolo I, Valerio AL, Leonardi A. Disinfection of ocular cells and tissues by atmospheric-pressure cold plasma. *Plos One*. 2012;7(3).
7. Isbary G, Morfill G, Schmidt HU, Georgi M, Ramrath K, Heinlin J, Karrer S, Landthaler M, Shimizu T, Steffes B, Bunk W, Monetti R, Zimmermann JL, Pompl R, Stolz W. A first pro-

- spective randomized controlled trial to decrease bacterial load using cold atmospheric argon plasma on chronic wounds in patients. *Brit J Dermatol.* 2010;163(1):78–82.
8. Daeschlein G, Scholz S, von Woedtke T, Junger M. Cold plasma antiseptics for skin and wounds: a new antimicrobial concept in dermatology. *Exp Dermatol.* 2012;21(3):e39.
  9. Hoentsch M, von Woedtke T, Weltmann KD, Nebe JB. Time-dependent effects of low-temperature atmospheric-pressure argon plasma on epithelial cell attachment, viability and tight junction formation in vitro. *J Phys D Appl Phys.* 2012;45(2).
  10. Haertel B, Wende K, von Woedtke T, Weltmann KD, Lindequist U. Non-thermal atmospheric-pressure plasma can influence cell adhesion molecules on HaCaT-keratinocytes. *Exp Dermatol.* 2011;20(3):282–4. Epub 2010/11/09.
  11. Kalghatgi S, Kelly CM, Cerchar E, Torabi B, Alekseev O, Fridman A, Friedman G, Azizkhan-Clifford J. Effects of non-thermal plasma on mammalian cells. *Plos One.* 2011;6(1):e16270. Epub 2011/02/02.
  12. Lange H, Foest R, Schafer J, Weltmann KD. Vacuum UV radiation of a plasma jet operated with rare gases at atmospheric pressure. *IEEE T Plasma Sci.* 2009;37(6):859–65.
  13. Bussiahn R, Kindel E, Lange H, Weltmann KD. Spatially and temporally resolved measurements of argon metastable atoms in the effluent of a cold atmospheric pressure plasma jet. *J Phys D Appl Phys.* 2010;43(16).
  14. Liu FX, Sun P, Bai N, Tian Y, Zhou HX, Wei SC, Zhou YH, Zhang J, Zhu WD, Becker K, Fang J. Inactivation of bacteria in an aqueous environment by a direct-current, cold-atmospheric-pressure air plasma microjet. *Plasma Process Polym.* 2010;7(3–4):231–6.
  15. Reuter S, Winter J, Schmidt-Bleker A, Schroeder D, Lange H, Knake N, Schulz-von der Gathen V, Weltmann KD. Atomic oxygen in a cold argon plasma jet: TALIF spectroscopy in ambient air with modelling and measurements of ambient species diffusion. *Plasma Sources Sci T.* 2012;21(2).
  16. Blackert S, Haertel B, Wende K, von Woedtke T, Lindequist U. Influence of non-thermal atmospheric pressure plasma on cellular structures and processes in human keratinocytes (HaCaT). *J Dermatol Sci.* 2013;70(3):173–81.
  17. Martínez-Ruiz A, Cadenas S, Lamas S. Nitric oxide signaling: classical, less classical, and nonclassical mechanisms. *Free Radic Biol Med.* 2011;51(1):17–29.
  18. Veal EA, Day AM, Morgan BA. Hydrogen peroxide sensing and signaling. *Molecular Cell.* 2007;26(1):1–14.
  19. Reuter S, Winter J, Schmidt-Bleker A, Tresp H, Hammer MU, Weltmann KD. Controlling the ambient air affected reactive species composition in the effluent of an argon plasma jet. *IEEE T Plasma Sci.* 2012;40(11):2788–94.
  20. Schmidt A, Wende K, Bekeschus S, Bundscherer L, Barton A, Ottmuller K, Weltmann KD, Masur K. Non-thermal plasma treatment is associated with changes in transcriptome of human epithelial skin cells. *Free Radical Res.* 2013;47(8):577–92.
  21. Boukamp P, Petrussevska RT, Breitkreutz D, Hornung J, Markham A, Fusenig NE. Normal keratinization in a spontaneously immortalized aneuploid human keratinocyte cell-line. *J Cell Biol.* 1988;106(3):761–71.
  22. Deyrieux AF, Wilson VG. In vitro culture conditions to study keratinocyte differentiation using the HaCaT cell line. *Cytotechnology.* 2007;54(2):77–83.
  23. Weltmann KD, Kindel E, von Woedtke T, Hahnel M, Stieber M, Brandenburg R. Atmospheric-pressure plasma sources: prospective tools for plasma medicine. *Pure Appl Chem.* 2010;82(6):1223–37.

24. Winter J, Wende K, Masur K, Iseni S, Dunnbier M, Hammer MU, Tresp H, Weltmann KD, Reuter S. Feed gas humidity: a vital parameter affecting a cold atmospheric-pressure plasma jet and plasma-treated human skin cells. *J Phys D Appl Phys*. 2013;46(29).
25. Cox J, Mann M. MaxQuant enables high peptide identification rates, individualized p.p.b.-range mass accuracies and proteome-wide protein quantification. *Nat Biotechnol*. 2008;26(12):1367–72.
26. Lackmann J-W, Schneider S, Edengeiser E, Jarzina F, Brinckmann S, Steinborn E, Havenith M, Benedikt J, Bandow JE. Photons and particles emitted from cold atmospheric-pressure plasma inactivate bacteria and biomolecules independently and synergistically. *J Royal Soc Interface*. 2013;10(89).
27. Geiger T, Wehner A, Schaab C, Cox J, Mann M. Comparative proteomic analysis of eleven common cell lines reveals ubiquitous but varying expression of most proteins. *Mol Cell Proteomics*. 2012;11(3).
28. Bundscherer L, Wende K, Ottmuller K, Barton A, Schmidt A, Bekeschus S, Hasse S, Weltmann KD, Masur K, Lindequist U. Impact of non-thermal plasma treatment on MAPK signaling pathways of human immune cell lines. *Immunobiology*. 2013;218(10):1248–55. Epub 2013/06/06.
29. Lanneau D, Brunet M, Frisan E, Solary E, Fontenay M, Garrido C. Heat shock proteins: essential proteins for apoptosis regulation. *J Cell Mol Med*. 2008;12(3):743–61.
30. Wende K, Strassenburg S, Haertel B, Harms M, Holtz S, Barton A, Masur K, von Woedtke T, Lindequist U. Atmospheric pressure plasma jet treatment evokes transient oxidative stress in HaCaT keratinocytes and influences cell physiology. *Cell Biol Int*. 2014;38(4):412–25. Epub 2013/10/25.
31. Vigh L, Maresca B, Harwood JL. Does the membrane's physical state control the expression of heat shock and other genes? *Trends Biochem Sci*. 1998;23(10):369–74.
32. Gorman AM, Szegezdi E, Quigney DJ, Samali A. Hsp27 inhibits 6-hydroxydopamine-induced cytochrome c release and apoptosis in PC12 cells. *Biochem Biophys Res Commun*. 2005;327(3):801–10.
33. Papaiahgari S, Zhang Q, Yleeberger SR, Cho HY, Reddy SP. Hyperoxia stimulates an Nrf2-ARE transcriptional response via ROS-EGFR-PI3K-Akt/ERK MAP kinase signaling in pulmonary epithelial cells. *Antioxid Redox Sign*. 2006;8(1–2):43–52.
34. Barton A, Wende K, Bundscherer L, Weltmann KD, Lindequist U, Masur K, editors. Non-thermal atmospheric pressure plasma treatment of human cells: The effect of ambient conditions. 21st Int Symp Plasma Chem; 2013; Cairns, Australia.